Int J Clin Exp Med 2018;11(3):1959-1972
www.ijcem.com /ISSN:1940-5901/IJCEM0063664

Original Article

iTRAQ-based proteomics analysis of hippocampus and striatum in rats with hyperglycemia and Parkinson's disease

Maierhaba[1], Xinling Yang[2], Mardan Mahmut[3], Yani Yao[1], Yumin Jia[1]

[1]*VIP Department of Internal Medicine, The First Affiliated Hospital of Xinjiang Medical University, Urumqi 830054, Xinjiang, China;* [2]*Department of Neurology, The Second Affiliated Hospital of Xinjiang Medical University, Urumqi 830028, Xinjiang, China;* [3]*Tumor Research Institute, The Affiliated Tumor Hospital of Xinjiang Medical University, Urumqi 830000, Xinjiang, China*

Received April 14, 2017; Accepted January 5, 2018; Epub March 15, 2018; Published March 30, 2018

Abstract: Background: This study is to investigate the differential protein expression patterns in hippocampus and striatum in rat models of Parkinson's disease (PD) and hyperglycemia (DM)-PD, and to elucidate the effects of hyperglycemia on PD pathogenesis. Methods: Rat models of hyperglycemia were induced by the high-fat and high-sugar diet combined with single intraperitoneal injection of streptozotocin. Then unilateral lesion with 6-OHDA was used to establish the DM-PD rat model. Differential proteins in the hippocampus and striatum of PD and DM-PD rats were analyzed by quantitative proteomics, with the iTRAQ technique combined with two-dimensional liquid chromatography-tandem mass spectrometry (2D LC-MS/MS). Protein expression was detected with Western blot analysis. Results: Totally 4988 proteins were identified. There were 463 differentially expressed proteins between the PD and DM-PD groups, including 281 up-regulated and 182 down-regulated proteins. Gene ontology (GO) functional analysis suggested that these differential proteins were mainly involved in the regulation of structural proteins, energy metabolism, and acute phase responses. Moreover, there were 32 different metabolic pathways screened in the DM-PD group. Proteins interaction network indicated that proteins of alpha B-crystallin, beta-crystallin A3, haptoglobin, FGG, and complexin-1 worked as the intersections. Similar results were obtained for the Western blot analysis. Conclusion: With the combination of iTRAQ and 2D LC-MS/MS, the main differential proteins in the hippocampus and striatum of DM-PD rats could be effectively screened, which might provide evidence for the prevention and treatment of diabetic PD in clinic.

Keywords: Parkinson's disease (PD), hyperglycemia, proteomics analysis, iTRAQ technology, 2D LC-MS/MS

Introduction

Effects of hyperglycemia on the nervous system are systematic, which could involve the central, peripheral, and autonomic nervous systems. Epidemiological surveys have shown that the blood sugar can aggravate the axial signs, rigidity, and tremor [1]. Compared with normal elderly people, the rates of muscle rigidity and gait abnormality are significantly higher in the elderly people suffering from hyperglycemia [2, 3]. Moreover, the cognitive function is also dramatically declined for diabetic patients compared with normal subjects [4-6]. Studies have shown that, for the early hyperglycemia (with no other complications), the risk of Parkinson's disease is 7 times higher [7] than the normal subjects. There is growing evidence that patients with Type 2 diabetes have an increased risk of developing Parkinson's disease and share similar dysregulated pathways, suggesting common underlying pathological mechanisms [8]. Mitochondrial dysfunction, abnormal protein aggregation, increased neuroinflammation, and impaired brain glucose metabolism are shared processes for insulin resistance, diabetes, and neurodegeneration, which have also been suggested as key players in the development of Parkinson's disease [9]. Insulin used to be solely considered as a peripherally acting hormone responsible for glucose homeostasis and energy metabolism. However accumulating evidence indicates insulin could cross the blood-brain-barrier and influence multiple

processes in brain, including the regulation of neuronal survival and growth, dopaminergic transmission, maintenance of synapses, and pathways involved in cognition. Growing evidence has shown that a process analogous to peripheral insulin resistance occurs in the brains of Parkinson's disease patients [10]. In recent years, a number of animal experiments, epidemiological studies, and clinical trials have shown the relationship between the hyperglycemia and the pathogenesis of Parkinson's disease (PD), which represents an important risk factor for the disease incidence [7, 11-14]. However, the mechanism underlying the effects of hyperglycemia on PD pathogenesis is still not clear.

Quantitative proteomics can accurately quantify and characterize all the proteins expressed by a genome. At present, the combination of iTRAQ labeling and 2D-LC-MS/MS is a hotspot field in quantitative proteomics. The iTRAQ labeling is characterized by the high sensitivity, fast response, complete labeling, and high repeatability [15, 16]. Over the past years, proteomics studies of PD have partially revealed the disease pathogenesis and suggested some key proteins that have not yet been identified.

To date, there are only few proteomics studies concerning the brain tissue of PD rats with hyperglycemia. To elucidate the mechanism of hyperglycemia on PD pathogenesis, the rat model of hyperglycemia-PD (DM-PD) was first established in this study. Then the main different proteins in the hippocampus and striatum between the PD and DM-PD rats were investigated by proteomic analysis, with the combination of iTRAQ and two-dimensional liquid chromatography-tandem mass spectrometry (2D LC-MS/MS) technologies.

Materials and methods

Rats

Totally 43 health SD rats (clean grade), weighing 200±10 g, were purchased from the Animal Center of the Xinjiang Medical University. These animals were kept at the temperature of 18-22°C, with the humidity of 50-60% and the day/night cycle of 12 h/12 h, as well as the free access to food and water. All animal experiments were conducted according to the ethical guidelines of the Second Affiliated Hospital of Xinjiang Medical University.

Model establishment

SD rats were fed standard diet for one week, and then randomly divided into the following groups: (1) the normal control (n = 3), sham-operated (n = 5), hyperglycemia (DM) (n = 10), PD (n = 10), and DM-PD (DM-PD) (n = 15) groups.

For the establishment of hyperglycemia rat model, diabetic rats were induced by high-fat and high-sugar diet combined with single intraperitoneal injection of streptozotocin. The basic diet consisted of 53% carbohydrate, 5% fat, and 23% protein. On the other hand, the high-fat and high-sugar diet was composed of 60% basic diet, added by 20% sucrose, 10% lard, 8% custard powder, and 2% cholesterol.

Totally 25 rats from the DM and DM-PD groups were fed on the high-fat and high-sugar diet for 4 weeks. Then these rats were subjected to the single intraperitoneal injection with 50 mg/kg streptozotocin. After 3 days, blood sample was obtained from the caudal vein, and the blood glucose was measured by the blood glucose meter. The hyperglycemia was confirmed when the random blood glucose was ≥ 16.7 mmol/L. After another 2 weeks, the blood sugar was tested again, and the high blood sugar levels proved the stable model establishment, which was suitable for the following experiments.

For the diabetic rats in the DM-PD group and the rats in the PD group, PD was induced by the by 6-OHDA unilateral lesion method. Briefly, the rats were anesthetized by the intraperitoneal injection of 30 mg/kg chloral hydrate, and then fixed on a stereotaxic apparatus. Right substania nigta pars compacta (SNc) and ventral tegmental (VTA) were located using the following coordinates: for SNc, 5.0±0.1 mm behind the bregma, 1.5±0.1 mm from sagittal suture on right, and 7.8±0.1 mm beneath dura mater; and for VTA, 4.6±0.1 mm behind the bregma, 0.9±0.1 mm from midline on right, and 7.3±0.1 mm beneath dura mater. After drilling the skull, 8 μg 6-OHDA (dissolved in 4 μL saline containing 0.2% ascorbic acid) was aspirated into a 10-μL micro-syringe, and carefully injected into the SNc and VTA, respectively. Four weeks later, the rats were intraperitoneally injected with 0.5 mg/kg apomorphine, and thereafter the rotating number within 10-40 min was recorded. Successful PD models were obtained when the constant rotating to the left was observed, with

the rotating frequency of >7 r/min (or 210 r/30 min). For the sham-operated group, the same procedures were performed, and only 4 μL saline containing 0.2% ascorbic acid was injected, without 6-OHDA. Rats in the normal control group received no drug treatments.

Tissue sample preparation

The rat models were anesthetized by intraperitoneal injection of 45 mg/kg chloral hydrate. After craniotomy, the brain was removed, and the bilateral hippocampi and striatum were isolated. The tissue samples were weighed and recorded, and stored at -80°C.

Protein preparation

Tissue samples were ground in liquid nitrogen, and extracted with the lysis buffer (7 M Urea, 2 M Thiourea, 4% CHAPS, and 40 mM Tris-HCl, pH 8.5) containing 1 mM PMSF and 2 mM EDTA. After 5 min, 10 mM DTT was added, and the suspension was sonicated at 200 W for 15 min, followed by centrifugation at 30000× *g*, at 4°C, for 15 min. The supernatant was mixed with 5× chilled acetone containing 10% (v/v) TCA, and the incubated at -20°C overnight. Then the mixture was subjected to the centrifugation at 30000× g at 4°C, and the supernatant was discarded. After washing with chilled acetone for three times, the precipitate was air-dried and dissolved in the lysis buffer (7 M Urea, 2 M Thiourea, 4% NP40, and 20 mM Tris-HCl, pH 8.0-8.5). The suspension was then sonicated at 200 W for 15 min, and centrifuged at 30000× *g*, at 4°C, for 15 min. The supernatant was the transferred to another tube, and 10 mM DTT was added, following by incubation at 56°C for 1 h. Subsequently, 55 mM IAM was use to incubate the supernatant in dark for 1 h. Then sample was mixed with 5× chilled acetone at -20°C for 2 h to precipitate proteins. After centrifugation at 30000× *g* at 4°C, the supernatant was discarded. The pellet was air-dried for 5 min, and then dissolved in 500 μL 0.5 M TEAB (Applied Biosystems, Milan, Italy). After sonication at 200 W for 15 min, the samples were centrifuged at 30000× *g* at 4°C for 15 min. The protein samples were kept at -80°C until further analysis.

iTRAQ Labeling and SCX fractionation

Totally 100 μg protein was digested with Trypsin Gold (Promega, Madison, WI, USA), with the protein to trypsin rate of 30:1, at 37°C for 16 h. After dried by vacuum centrifugation, the peptides were reconstituted in 0.5 M TEAB and the processed with the 8-plex iTRAQ reagent (Applied Biosystems), according to the manufacturer's instructions. Briefly, 1 unit iTRAQ reagent was thawed and reconstituted in 24 μL isopropanol. Samples were labeled with the iTRAQ tags. The peptides were labeled with the isobaric tags, and incubated at room temperature for 2 h, which were then pooled and dried by vacuum centrifugation.

SCX chromatography was performed with a LC-20AB HPLC Pump system (Shimadzu, Kyoto, Japan). The iTRAQ-labeled peptides were reconstituted with 4 mL buffer A (25 mM NaH_2PO_4 in 25% ACN, pH 2.7) and loaded onto a 4.6×250 mm Ultremex SCX column containing 5-μm particles (Phenomenex). The peptides were eluted with a gradient of buffer A for 10 min, 5-60% buffer B (25 mM NaH_2PO_4 and 1 M KCl in 25% ACN, pH 2.7) for 27 min, 60-100% buffer B for 1 min, at the flow rate of 1 mL/min. The system was maintained in 100% buffer B for 1 min, and then equilibrated for 10 min, prior to the next injection. Elution was monitored by measuring the absorbance at 214 nm, and fractions were collected every 1 min. Eluted peptides were pooled into 20 fractions, and desalted with a Strata X C18 column (Phenomenex) and dried in vacuum.

LC-ESI-MS/MS analysis

Each fraction was re-suspended in buffer A (5% CAN and 0.1% FA), and centrifuged at 20000× *g* for 10 min, to obtain the final peptide concentration of about 0.5 μg/μL. Totally 10 μL supernatant was loaded on a LC-20AD nanoHPLC (Shimadzu, Kyoto, Japan) onto a 2-cm C18 trap column. Then the peptides were eluted onto a 10-cm analytical C18 column (with the inner diameter of 75 μm). Samples were loaded at 8 μL/min for 4 min, and then gradient was run at 300 nL/min for 35 min, starting from 2%-35% B (95% ACN and 0.1% FA), followed by linear gradient to 60% within 5 min, linear gradient to 80% within 2 min, maintenance at 80% B for 4 min, and finally returning to 5% within 1 min.

Data acquisition was performed with a TripleTOF 5600 System (AB SCIEX, Concord, ON) fitted with a Nanospray III source (AB SCIEX, Concord, ON) and a pulled quartz tip as the emitter (New Objectives, Woburn, MA). Data was acquired

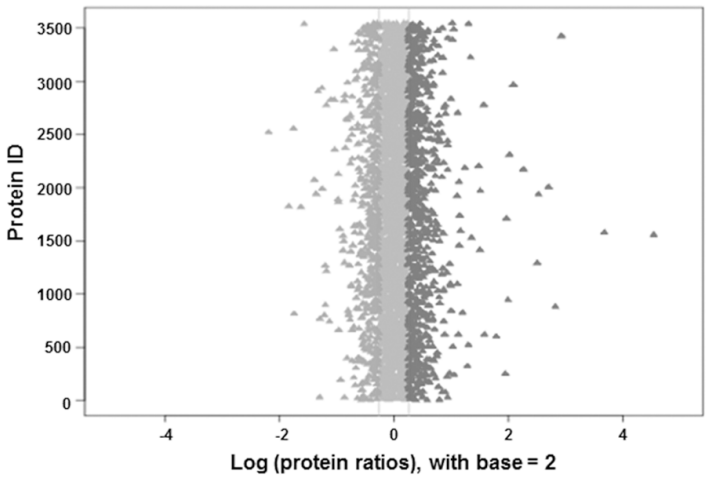

Figure 1. Protein abundance ratio distribution of PD and DM-PD groups. Totally 463 proteins were quantified (I ratio >1.2 or ≤0.6) in the PD and DM-PD groups (281 up-regulated and 182 down-regulated proteins in the DM-PD group).

with the ion spray voltage of 2.5 kV, curtain gas of 30 psi, nebulizer gas of 15 psi, and interface heater temperature of 150. MS was operated with a RP of ≥ 30000 FWHM for TOF MS scan. For IDA, survey scans were acquired in 250 ms, and as many as 30 product ion scans were collected if the threshold of 120 counts/s was exceeded, with a 2+-5+ charge-state. Total cycle time was fixed to 3.3 s. Q2 transmission window was 100 Da for 100%. Four time bins were summed for each scan at the pulse frequency of 11 kHz, through monitoring of the 40-GHz multichannel TDC detector with four-anode channel detect ion. Sweeping collision energy of 35±5 eV coupled with iTRAQ adjust rolling collision energy was applied to all precursor ions for collision-induced dissociation. Dynamic exclusion was set for 1/2 of the peak width (15 s), and then the precursor was refreshed off the exclusion list.

Western blot analysis

Protein samples were obtained as described above. Totally 50 μg protein was loaded in each lane and subjected to SDS-PAGE, and then transferred onto the PVDF membrane. After blocking with 5% non-fat milk for 1 h, the membrane was incubated with chicken anti-CPLX1 (1:500 dilution; ab15855; Abcam, Cambridge, MA, USA), rabbit anti-Fibrinogen gamma chain (1:400 dilution; ab62527; Abcam), rabbit anti-alpha B-crystallin (1:500 dilution; ab76467; Abcam), rabbit anti-beta-crystallin A3 (1:400 dilution; ab151722; Abcam), rabbit anti-haptoglobin (1:500 dilution; ab131236; Abcam), rabbit anti-ACTB (1:500 dilution; ab8226; Abcam) primary antibodies, respectively, at 4°C overnight. After washing, the membrane was incubated with the secondary antibody (1:10000 dilution) at 37°C for 1 h. Color development was performed with the ChemiScope mini chemiluminescence method, in which the solutions A and B were mixed and used to incubate the membrane.

Statistical analysis

Raw data acquired from the Orbitrap were converted into MGF files using the Proteome Discoverer 1.2 (5600 msconverter; Thermo). Protein identification was performed using the Mascot search engine (version 2.3.02; Matrix Science, London, UK) against database. For protein identification, 0.05 Da (2ppm) mass tolerance was permitted for intact peptide masses and 0.05 Da for fragmented ions, allowing for one missed cleavage in the trypsin digests. Gln->pyro-Glu (N-term Q), Oxidation (M), and Deamidated (NQ) represented the potential variable modifications, while the Carbamidomethyl (C), iTRAQ8plex (N-term), and iTRAQ8plex (K) were the fixed modifications. The peptide charge states were set to +2 and +3. In particular, automatic search against decoy database was performed in the Mascot, choosing the decoy checkbox in which random sequence is generated and tested for raw spectra and the real database. To reduce the probability of false identification, only peptides with 95% confidence interval in the Mascot probability analysis (greater than "identity") were considered as identified. Confident protein identification involved at least one unique peptide. For protein quantification, the protein should contain at least two unique spectra. Quantitative protein ratios were weighted and normalized by the median ratio in Mascot. Only ratios with $P < 0.05$ were used herein, and only fold changes of >1.2 were considered as statistically significant.

Results

Model establishment and behavioral observation

During the model establishment, one rat in the sham-operated group and three rats in the hyperglycemia group failed to survive. There

Table 1. Differentially expressed proteins between PD and DM-PD rats

Accession No.	Description	Cov	PD vs.DM-PD
tr|M0R9G2|M0R9G2_RAT	Protein LOC100911545	4.1	7.652
tr|Q5PQU1|Q5PQU1_RAT	Kininogen 1	15.8	6.553
tr|E0A3N4|E0A3N4_RAT	Serpina3n-like protein	17	5.714
sp|P10066|CRGB_RAT	Gamma-crystallin B	34.9	4.825
sp|P56374|CRBA4_RAT	Beta-crystallin A4	27.6	4.085
tr|P70621|P70621_RAT	Calcium/calmodulin-dependent protein kinase II gamma E-subunit (Fragment) = 1	37.3	4.006
sp|P06866|HPT_RAT	Haptoglobin	25.9	3.932
sp|P02523|CRBB1_RAT	Beta-crystallin B1	24	3.882
sp|P14881|CRBA1_RAT	Beta-crystallin A3	12.1	3.013
tr|M0R5T4|M0R5T4_RAT	Protein Rac3 (Fragment)	17.8	2.99
tr|Q6AY99|Q6AY99_RAT	Aldo-keto reductase family 1, member B10 (Aldose reductase)	25.6	2.852
tr|A0JN13|A0JN13_RAT	Crystallin, alpha A	22.5	2.812
tr|M0RAK2|M0RAK2_RAT	Protein LOC684270	8.4	2.576
sp|P61206|ARF3_RAT	ADP-ribosylation factor 3	58.6	2.481
tr|E9PT53|E9PT53_RAT	Protein Wfs1	13.4	2.376
sp|P23928|CRYAB_RAT	Alpha-crystallin B chain	18.3	2.313
sp|P51907|EAA3_RAT	Excitatory amino acid transporter 3	3.4	2.085
sp|P02680|FIBG_RAT	Fibrinogen gamma chain	12.4	2.043
sp|Q9QZ76|MYG_RAT	Myoglobin	21.4	0.221
sp|P31421|GRM2_RAT	Metabotropic glutamate receptor 2	6.9	0.282
tr|F1LM05|F1LM05_RAT	Protein LOC299282	19.5	0.301
sp|P04177|TY3H_RAT	Tyrosine 3-monooxygenase	22.5	0.326
sp|P14046|A1I3_RAT	Alpha-1-inhibitor 3	17.9	0.34
sp|P00564|KCRM_RAT	Creatine kinase M-type	23.9	0.402
tr|Q8CHN7|Q8CHN7_RAT	Neuron-specific protein PEP-19	28.7	0.439
tr|F1LX13|F1LX13_RAT	cAMP and cAMP-inhibited cGMP 3,5-cyclic phosphodiesterase 10A (Fragment)	6.7	0.462
sp|P63041|CPLX1_RAT	Complexin-1	33.6	0.487

were finally 7 rat models (70%) in the in the DM group, 6 rat models (60%) in the PD group, and 8 rat models (53.3%) in the DM-PD group. For the PD group, on day 2 after 6-OHDA injection, some rats exhibited body imbalance, accompanied with piloerection, skewed head and body, slow and reduced movement, lifted forelimbs, and washing and foraging actions. Moreover, the forelimb on the impaired side was addicted, while the forelimb on the contralateral side was outstretched. Furthermore, these rats displayed back arch, tail stiffness, slow movement, and irritability. On day 5 to 7 after injection, several animals showed skewed head and body to the injection side. These results suggest that the models are stable and suitable for the following investigation.

Protein screening and expression analysis

Based on the analysis of iTRAQ labeling and 2D LC-MS/MS, totally 4988 proteins were identified in these 5 groups. For the relative quantification, the proteins were screened with the two-sample *t*-test and the difference multiple comparison method. The protein abundance ratio was close to 1 when the amount of the same protein in two samples did not change significantly. When the abundance ratio (i.e., the difference multiple) reached 1.2, with $P < 0.05$, differential proteins were confirmed and identified. The distribution of protein abundance ratios was shown in **Figure 1**. As shown in **Table 1**, there were totally 463 quantified proteins (I ratio >1.2 or ≤0.6) in the PD and DM-PD groups, in which there were 281 up-regulated and 182 down-regulated proteins in the DM-PD group. For the more stringent quantitative criteria (I ratio >1.5 or ≤0.5), totally 27 proteins were recognized, which there were 18 up-regulated and 9 down-regulated proteins in the DM-PD group. These results suggest that hyperglycemia can induce protein changes in hippocampus and striatum of rats, leading to abnormal aggregation of proteins or decreased synthesis of related proteins.

GO and COG annotation analyses

The GO database provided the information describing the gene molecular functions, cellular components, and biological processes. In

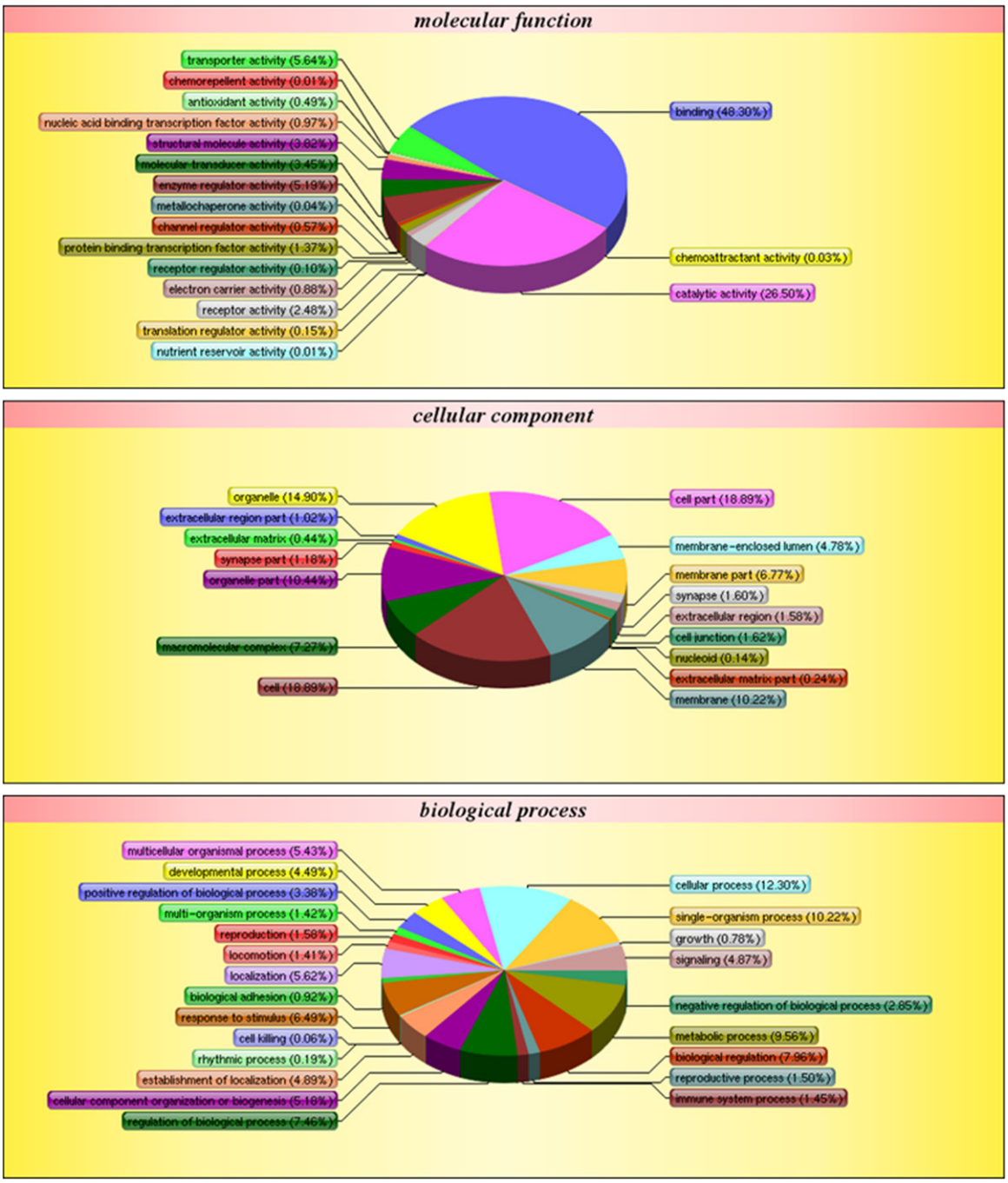

Figure 2. GO classification for protein screening. For the molecular function analysis, mainly the binding (48.8%) and catalytic activity (28.5%) proteins were implied. For the cellular component analysis, the cell part (18.89%) and organelle (14.9%) proteins were included. For the biological process analysis, the cellular process (12.30%), single-organism process (10.22%), and metabolic process (9.56%) were involved.

this study, GO annotation was used to explore the combination of single and multiple functions associated with differential gene expressions. Our results showed that the all the function characteristics were involved in the GO classification. As shown in **Figure 2**, for the molecular function analysis, mainly the binding (48.8%) and catalytic activity (28.5%) proteins were implied. Moreover, for the cellular component analysis, the cell part (18.89%) and organelle (14.9%) proteins were included. Furthermore, for the biological process analysis, the

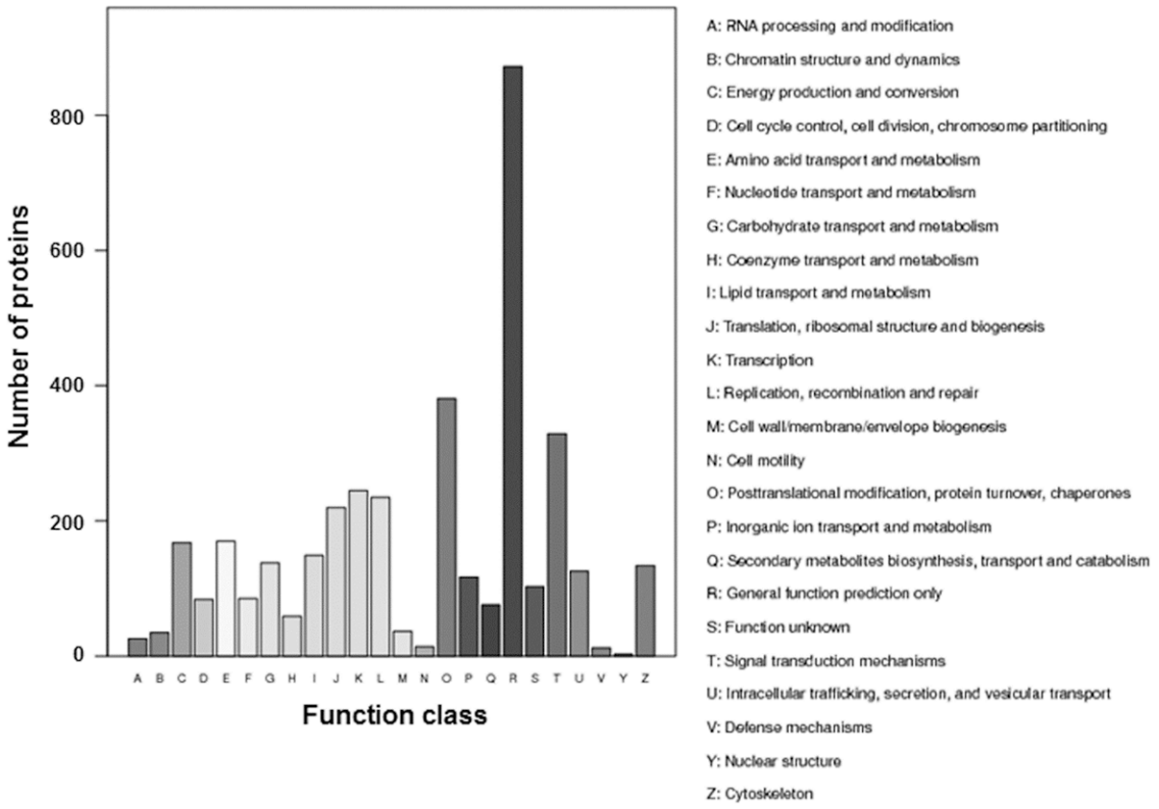

Figure 3. COG annotation for protein screening. Orthologous classification of proteins was performed based on the Cluster of Orthologous Groups (COG) database. The identified proteins were compared with the COG database, and the possible functions of these proteins were predicted, followed by the functional classification.

cellular process (12.30%), single-organism process (10.22%), and metabolic process (9.56%) were involved.

On the other hand, the orthologous classification of proteins was performed based on the Cluster of Orthologous Groups (COG) database. The identified proteins were compared with the COG database, and the possible functions of these proteins were predicted, followed by the functional classification (**Figure 3**). Taken together, these results suggest that the biological functions of the detected differential proteins include molecular chaperones, signal transduction, protein replication, gene transcription and translation, energy metabolism, amino acid metabolism, as well as lipid and carbohydrate transportation and metabolism.

GO enrichment analysis

All the identified differential proteins were mapped to each term in the Gene Ontology database (http://geneontology.org/), and the proteins for each term were counted. Based on the hypergeometric test, the GO terms significantly enriched in differential proteins compared with the protein background. GO terms with $P \leq 0.05$ were defined as significant enrichment of differential proteins. GO significance analysis would contribute to determine the main biological functions of differential proteins. For the molecular function, there were 65 major GO terms, including transporter activity (13.6%), enzyme binding (15.5%), and receptor binding (11.5%). Moreover, for the cellular component, there were 92 major GO terms, including organelle (78.7%), cytoplasm (82.1%), intracellular organelle (78.7%), membrane (56.6%), and intracellular organelle part (57.3%). Furthermore, for the involved biological processes, major differential GO terms included single-organism cellular process (72.8%), multicellular organismal process (44.1%), single-multicellular organism process (43.6%), cellular component organization or biogenesis (39.8%), cellular component organization (39%), signaling (34.75), and single organism signaling (34.7%). These results suggest that these differential

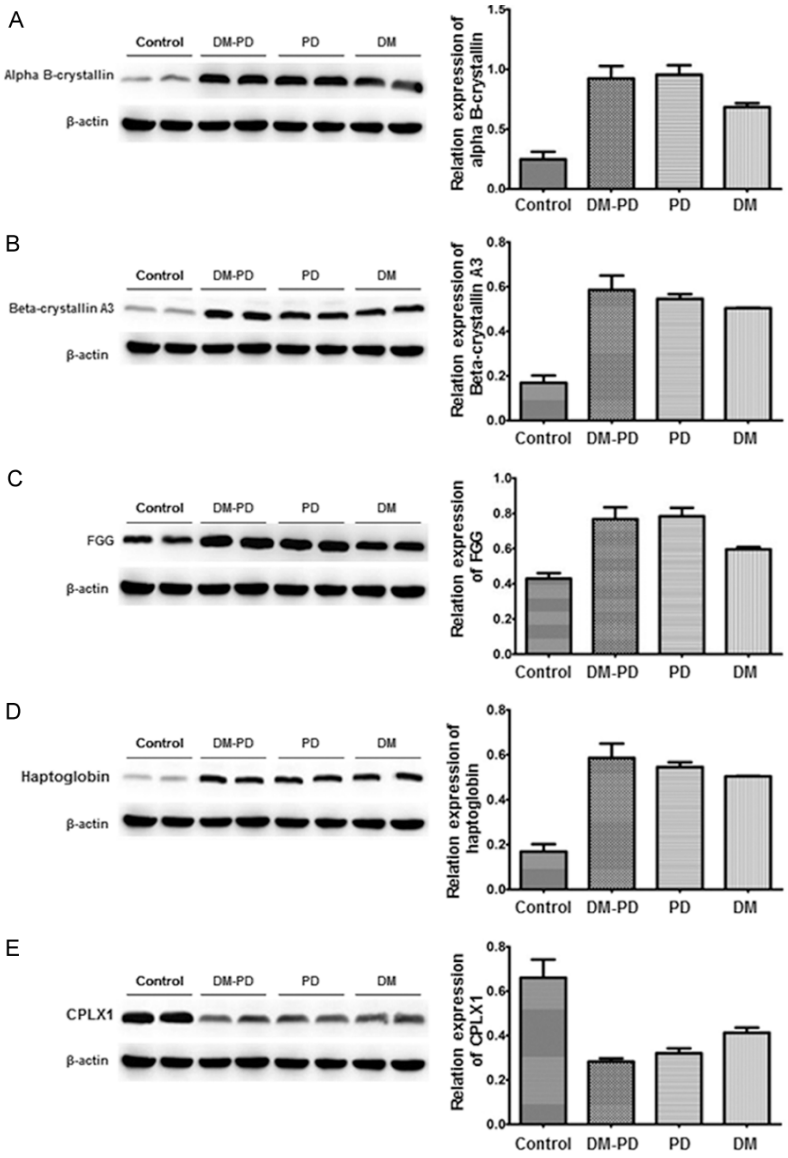

Figure 4. Western blot analysis. (A-D) Compared with the normal control group, the expression levels of alpha B-crystallin (A), beta-crystallin A3 (B), FGG (C), and haptoglobin (D) were significantly up-regulated in the hyperglycemia, DM-PD, and PD groups. (E) Compared with the normal control group, the complexin-1 (CPLX1) expression levels in the hyperglycemia, DM-PD, and PD groups were significantly down-regulated.

proteins are mainly involved in the regulation of structural proteins, energy metabolism, acute phase responses, and signaling transduction.

Metabolic pathway annotation analysis

Pathway enrichment analysis was based on the KEGG Pathway, using the hypergeometric test, in which all the identified proteins were compared with the protein background, and the pathways enriched in differential proteins were confirmed. The pathway significant enrichment analysis could determine the major biochemical metabolic pathways and signals involving the differential proteins. Our results showed that, there totally 201 related pathways in the comparison between the PD and DM-PD groups. Moreover, 32 pathways were enriched in differential proteins ($P < 0.05$), including the dopaminergic synapse, glutamatergic synapse, Parkinson's disease, MAPK signaling pathway, calcium signaling pathway, serotonergic synapse, and Fc gamma R-mediated phagocytosis. These findings suggest that hyperglycemia might lead to excitatory amino acid transportation, which is closely related to pathogenesis of Parkinson's disease (excitotoxicity), as well as differential expression levels of free radical scavenging and oxidative stress-related proteins.

Western blot analysis

Based on the protein-protein interaction network and STRING searching, the alpha B-crystallin, beta-crystallin A3, haptoglobin, FGG, and complexin-1 had been found to be located at the interaction network intersections, indicating that these candidate proteins might play important roles in the disease pathogenesis and development. Then Western blot analysis was performed to confirm these findings (**Figure 4**). Our results showed that, compared with the normal control group, the expression levels of alpha B-crystallin, beta-crystallin A3, FGG, and haptoglobin were significantly up-regulated in the hyperglycemia, DM-PD, and PD groups. Similar results were obtained for the iTRAQ proteomics analysis, which suggested the up-regu-

lated expression levels of these proteins in the experimental groups. On the other hand, compared with the normal control group, the complexin-1 (CPLX1) expression levels in the hyperglycemia, DM-PD, and PD groups were significantly down-regulated. Similar results were obtained for the iTRAQ proteomics analysis. These results suggest that the proteomics analysis can provide satisfactory reliability and accuracy.

Discussion

Hyperglycemia is a metabolic disease is induced by abnormal production and action of insulin, which is characterized by hyperglycemia. The impact of hyperglycemia on the nervous system is systematic, and the central nervous system would be also involved. Studies have shown that, for the early hyperglycemia (with no other complications), the risk of Parkinson's disease is 7 times higher [7], and the risk of Alzheimer's disease is 2 times higher [17], than the normal control subjects. The mechanisms of hyperglycemia leading to increased incidence of Parkinson's disease are still not fully elucidated. Studies have shown that it may be mainly related to the metabolic disorders in hyperglycemia caused by oxidative stress, protein function alterations, or abnormal protein aggregation.

Quantitative proteomics can accurately quantify and characterize all the proteins expressed by a genome. At present, the combination of iTRAQ labeling and 2D-LC-MS/MS is a hotspot field in quantitative proteomics. The iTRAQ labeling is characterized by the high sensitivity, fast response, complete labeling, and high repeatability [15, 16]. In order to investigate the mechanism underlying the pathogenesis of hyperglycemia-induced increased risk of Parkinson's disease, in this study, the rat model of DM-PD was established, and totally 4988 proteins in the hippocampal and striatal tissues were identified by the iTRAQ labeling combined with 2D-LS-MS/MS proteomics technology. Compared with the PD group, there were 463 differential proteins in the DM-PD group, including 181 down-regulated and 282 up-regulated proteins. The up-regulated proteins were mainly the cell structure protein, energy metabolism, and acute phase reaction proteins, which met the energy demand after the stimulation. On the other hand, the down-regulated proteins were mainly proteins involved in the cell energy metabolism, especially associated with the synaptic proteins. GO molecular functional analysis showed that the differential proteins were mainly structural proteins or involved in the cell differentiation process, or participating in the interaction of enzymes. These findings provide evidence for the investigation of mechanism of hyperglycemia-induced higher risk of PD. The STRING searching showed that proteins such as alpha B-crystallin, Beta Crystallin A3, haptoglobin, FGG, and complexin-1 were at the intersections of the interaction network of differentially expressed proteins. These results suggest that these five candidate proteins may play important roles in the disease occurrence and development. Western blot analysis further showed the same expression trends of the candidate proteins in the DM-PD and PD groups, which were consistent with the results of mass spectrometry, suggesting the result reliability.

Alpha B-crystallin is a water-soluble protein easily found in the lens epithelial cells, which belongs to the heat shock protein family. It has been found, alpha B-crystallin is highly expressed in the heart, skeletal muscle, and kidney tissues, as well as in the neurological diseases. Under the condition of infection, ischemia, hypoxia and oxidative stress, the expression level of alpha B-crystallin would be changed to exert protective effects. When stress and pathological changes occur, they could prevent the programmed cell death and protein denaturation [18-20]. Alpha B-crystallin is also a potential reverse regulatory factor, which can block the immune pathways in the immune and central nervous systems [21]. Ousman *et al.* [22] have found that knockout of alpha B-crystallin could increase the immune system activity in mice, with up-regulated expression of caspase-3 and increased glial cell apoptosis, suggesting that alpha B-crystallin is closely linked with cellular apoptosis. Some neurological diseases, such as Alzheimer's disease and Parkinson's disease, are always related to the abnormal aggregation of alpha B-crystallin in the nervous system. Skrzydlewska *et al.* [23] have found that, under oxidative stress, the activities of antioxidant enzymes, such as superoxide dismutase (SOD) and glutathione peroxidase (GPx), would be declined in the body. Moreover, Masilamoni *et al.* [24] have shown that alpha B-crystallin can maintain the activities of SOD, glutathione (GSH), and the

related enzymes, in the antioxidant enzyme system, exerting protective effects. Lewy bodies are the typical pathologic features of Parkinson's disease. The major components of Lewy bodies represent the abnormally accumulated α-synuclein, which is also the main cause for the neurodegenerative alterations in Parkinson's disease. It has been shown that, through binding α-synuclein, alpha B-crystallin would inhibit the elongation of amyloid fiber, prevent the abnormal fiber aggregation, and limit the occurrence of protein misfolding. In this study, the expression level of alpha B-crystallin was significantly elevated in the hyperglycemia group. Considering its relationship with hyperglycemia-induced oxidative stress, hyperglycemia might aggravate the oxidative stress in the brains of PD rats.

In more than 51000 PD-related studies, totally 4121 proteins have been involved [25]. The 2-DE map analysis of the PD patients have suggested 35 PD-related proteins, in which 9 proteins have been considered as closely related to the disease pathogenesis, including the haptoglobin (HP), thyroxine, apolipoprotein A-1, serum amyloid P component, apolipoprotein E, factor H, fibrinogen γ, thrombin, and complement C3 [26]. Haptoglobin (HP), an acute phase serum protein, has high affinity for free hemoglobin (Hb) [27, 28]. The Hp-hemoglobin complex is cleared in the liver by monocytes and macrophages via the CD163 receptor-mediated endocytosis [29], which is involved in the clearance of free Hb and the damage neutralization in oxidative stress. HP closely binds to hemoglobin, and HP-hemoglobin participates in the regulation of iron metabolism and serum iron content [30]. The binding globin consists of two distinct polypeptide chains, i.e, the α and β chains. There are three distinct subtypes (HP 1-1, HP 2-1, and HP 2-2), which are distinctly different in structure and function [31]. In a study concerning PD, HP 2-1 has been shown to increase the risk of PD, mainly associated with iron metabolic abnormality [32]. It has also been confirmed that the HP 2-1 subtype is closely linked with the occurrence of sporadic PD cases [33]. In the past two decades, a number of studies have suggested that the genetic polymorphisms in HP are closely related to hyperglycemia-related complications [34, 35]. HP 1-1 genotype has been associated with the cognitive impairments in elderly diabetic cases [36], including endothelial injury, abnormal neovascularization, and ineffective blood-brain-barrier [37]. The HP 1-1 genotype may be involved in the endothelial repairing process, reducing the activities of epithelial progenitor cells [38].

Studies have shown that, in males older than 7 years, the blood levels of high fibrinogen are associated with increased risk of PD [39]. Fibrinogen is composed of three pairs of non-identical polypeptide chains, and the A, B and C chains are the components of the serum glycoprotein [40]. The 2-DE map and Western blot analyses of PD patient serum have shown significantly increased serum fibrinogen C chain. Proteomics analysis of lymphocytes in patients with Parkinson's disease has found that the two different subtypes of γ-fibrinogen [FGG] are associated with the clinical manifestations and disease duration of PD [41]. FGG is not produced by lymphocytes, but FGG isoforms bind tightly to the lymphocyte-specific receptors and regulate the lymphocyte activity [42]. Therefore, the over-expression of FGG isoforms in serum may be closely related to the pathological changes of PD. In serum, FGG participates in the fibrin polymerization and cross-linking, initiating of fibrinolysis. It also regulates the XIII activity, providing high-affinity binding sites for platelets and leukocytes, modulating the binding of prothrombin to fibrin [43]. FGG has been recognized as the marker for the evaluation of thrombosis and inflammatory responses [44], which may play a role in the neurodegenerative diseases [45, 46]. Several animal experiments and clinical studies have confirmed that FGG is involved in the pathogenesis of by cardiovascular and cerebrovascular diseases induced by smoking, hyperlipidemia, and hyperglycemia [47]. Hyperglycemia-induced hyperinsulinemia, insulin resistance, and inflammatory factor elevation (such as FGG) may aggravate the cerebrovascular diseases, thus affecting the brain and central nervous system damages [48]. Recent studies have shown that the advanced glycation end products (AGEs) bind to plasma membrane-specific receptors to change the intracellular signaling, gene expression, and release of pro-inflammatory molecules and free radicals. Glycosylated plasma proteins (such as FGG) can combine to form different types of AGEs, participating in the diabetic complications including neuropathy [49].

The release of neurotransmitters between synapses is accomplished by interactions of hundreds of proteins. Complexin-1 is an important cytoplasmic protein that plays a coordinating role in the release of neurotransmitters [50]. Glutamate, an important excitatory neurotransmitter, exerts important physiological functions in the central nervous system. However, excessive glutamate produces excitatory neurotoxins [51, 52]. Under physiological conditions, glutamic acid is released by the soluble N-ethylmaleimide-sensitive factor attachment protein receptor (SNARE) complex through the calcium-dependent cytokine efflux. The SNARE complex is composed of the synaptic vesicle protein, synaptic membrane protein SNAP25, and synaptic fusion protein-1, which regulates multiple protein process via the vesicle fusion and release of neurotransmitters, in which complexin protein family plays an important regulatory role [53, 54]. Complexin binds to the SNARE complex, which regulates the release of neurotransmitters [55, 56]. Complexin I is mainly expressed in ends of synapses, which is related to the release of inhibitory neurotransmitter aminobutyric acid. It has been reported that when the level of complexins expression changes, the synapse transmission and neurotransmitter release would be changed, which is associated with the pathogenesis of Huntington's disease, Parkinson's disease, Alzheimer's disease, and traumatic brain injuries [57]. Complexins-mediated neurotransmitter release process is regulated by the NADPH oxidase NOX2 [55, 58]. Our results showed that, the expression levels of complexins were significantly reduced in the hippocampus and striatum in diabetic rats. Hyperglycemia may affect the function of complexins by influencing oxidases (such as NADPH).

Conclusion

In conclusion, the assessment of proteins in the rat hippocampus and striatum and the analyses of pathway metabolism were performed. Our results showed that the differential metabolic pathways between DM-PD and PD groups included the dopamine metabolism, glutamate metabolism, and calcium signal transduction pathways, which were closely related to the occurrence of PD. These findings suggest that hyperglycemia might lead to excitatory amino acid transporters closely related to pathogenesis of Parkinson's disease (excitotoxicity), differential expression levels of free radical scavenging and oxidative stress-related proteins, and changes of the cellular structural proteins in the hippocampus and striatum. These findings might contribute to the investigation of the prevention and treatment of diabetic PD in clinic.

Acknowledgements

This work was supported by the Natural Science Foundation of Xinjiang Uygur Autonomous Region [grant number 2015211c060].

Disclosure of conflict of interest

None.

Address correspondence to: Xinling Yang, Department of Neurology, The Second Affiliated Hospital of Xinjiang Medical University, No. 38, South Lake Road, Urumqi 830028, Xinjiang, China. Tel: 86-131 39699251; E-mail: poplar862@sohu.com; m1870-3025906@163.com

References

[1] Wilson RS, Schneider JA, Bienias JL, Evans DA and Bennett DA. Parkinsonianlike signs and risk of incident Alzheimer disease in older persons. Arch Neurol 2003; 60: 539-544.

[2] Cereda E, Barichella M, Cassani E, Caccialanza R and Pezzoli G. Clinical features of Parkinson disease when onset of diabetes came first: a case-control study. Neurology 2012; 78: 1507-1511.

[3] Arvanitakis Z, Wilson RS, Schneider JA, Bienias JL, Evans DA and Bennett DA. Diabetes mellitus and progression of rigidity and gait disturbance in older persons. Neurology 2004; 63: 996-1001.

[4] Luchsinger JA, Reitz C, Patel B, Tang MX, Manly JJ and Mayeux R. Relation of diabetes to mild cognitive impairment. Arch Neurol 2007; 64: 570-575.

[5] Schnaider Beeri M, Goldbourt U, Silverman JM, Noy S, Schmeidler J, Ravona-Springer R, Sverdlick A and Davidson M. Diabetes mellitus in midlife and the risk of dementia three decades later. Neurology 2004; 63: 1902-1907.

[6] Ahtiluoto S, Polvikoski T, Peltonen M, Solomon A, Tuomilehto J, Winblad B, Sulkava R and Kivipelto M. Diabetes, Alzheimer disease, and vascular dementia: a population-based neuropathologic study. Neurology 2010; 75: 1195-1202.

[7] Hu G, Jousilahti P, Bidel S, Antikainen R and Tuomilehto J. Type 2 diabetes and the risk of Parkinson's disease. Diabetes Care 2007; 30: 842-847.
[8] Athauda D and Foltynie T. Insulin resistance and Parkinson's disease: a new target for disease modification? Prog Neurobiol 2016; 145-146: 98-120.
[9] Lenart N, Brough D and Denes A. Inflammasomes link vascular disease with neuroinflammation and brain disorders. J Cereb Blood Flow Metab 2016; 36: 1668-1685.
[10] Ashraghi MR, Pagano G, Polychronis S, Niccolini F and Politis M. Parkinson's disease, diabetes and cognitive impairment. Recent Pat Endocr Metab Immune Drug Discov 2016; 10: 11-21.
[11] Morris JK, Bomhoff GL, Stanford JA and Geiger PC. Neurodegeneration in an animal model of Parkinson's disease is exacerbated by a high-fat diet. Am J Physiol Regul Integr Comp Physiol 2010; 299: R1082-1090.
[12] Morris JK, Bomhoff GL, Gorres BK, Davis VA, Kim J, Lee PP, Brooks WM, Gerhardt GA, Geiger PC and Stanford JA. Insulin resistance impairs nigrostriatal dopamine function. Exp Neurol 2011; 231: 171-180.
[13] Cereda E, Barichella M, Pedrolli C, Klersy C, Cassani E, Caccialanza R and Pezzoli G. Diabetes and risk of Parkinson's disease: a systematic review and meta-analysis. Diabetes Care 2011; 34: 2614-2623.
[14] Schernhammer E, Hansen J, Rugbjerg K, Wermuth L and Ritz B. Diabetes and the risk of developing Parkinson's disease in Denmark. Diabetes Care 2011; 34: 1102-1108.
[15] Martyniuk CJ, Alvarez S and Denslow ND. DIGE and iTRAQ as biomarker discovery tools in aquatic toxicology. Ecotoxicol Environ Saf 2012; 76: 3-10.
[16] Schwacke JH, Hill EG, Krug EL, Comte-Walters S and Schey KL. iQuantitator: a tool for protein expression inference using iTRAQ. BMC Bioinformatics 2009; 10: 342.
[17] Driver JA, Smith A, Buring JE, Gaziano JM, Kurth T and Logroscino G. Prospective cohort study of type 2 diabetes and the risk of Parkinson's disease. Diabetes Care 2008; 31: 2003-2005.
[18] Gangadhariah MH, Wang B, Linetsky M, Henning C, Spanneberg R, Glomb MA and Nagaraj RH. Hydroimidazolone modification of human alphaA-crystallin: effect on the chaperone function and protein refolding ability. Biochim Biophys Acta 2010; 1802: 432-441.
[19] Kase S, He S, Sonoda S, Kitamura M, Spee C, Wawrousek E, Ryan SJ, Kannan R and Hinton DR. alphaB-crystallin regulation of angiogenesis by modulation of VEGF. Blood 2010; 115: 3398-3406.
[20] Andley UP, Song Z, Wawrousek EF, Fleming TP and Bassnett S. Differential protective activity of alpha A- and alphaB-crystallin in lens epithelial cells. J Biol Chem 2000; 275: 36823-36831.
[21] Cherneva RV, Georgiev OB, Petrova DS, Trifonova NL, Stamenova M, Ivanova V and Vlasov VI. The role of small heat-shock protein alphaB-crystalline (HspB5) in COPD pathogenesis. Int J Chron Obstruct Pulmon Dis 2012; 7: 633-640.
[22] Ousman SS, Tomooka BH, van Noort JM, Wawrousek EF, O'Connor KC, Hafler DA, Sobel RA, Robinson WH and Steinman L. Protective and therapeutic role for alphaB-crystallin in autoimmune demyelination. Nature 2007; 448: 474-479.
[23] Skrzydlewska E and Farbiszewski R. Glutathione consumption and inactivation of glutathione-related enzymes in liver, erythrocytes and serum of rats after methanol intoxication. Arch Toxicol 1997; 71: 741-745.
[24] Masilamoni JG, Jesudason EP, Bharathi SN and Jayakumar R. The protective effect of alpha-crystallin against acute inflammation in mice. Biochim Biophys Acta 2005; 1740: 411-420.
[25] Mourad N, Mounier N, Briere J, Raffoux E, Delmer A, Feller A, Meijer CJ, Emile JF, Bouabdallah R, Bosly A, Diebold J, Haioun C, Coiffier B, Gisselbrecht C and Gaulard P. Clinical, biologic, and pathologic features in 157 patients with angioimmunoblastic T-cell lymphoma treated within the Groupe d'Etude des Lymphomes de l'Adulte (GELA) trials. Blood 2008; 111: 4463-4470.
[26] Alberio T, Bucci EM, Natale M, Bonino D, Di Giovanni M, Bottacchi E and Fasano M. Parkinson's disease plasma biomarkers: an automated literature analysis followed by experimental validation. J Proteomics 2013; 90: 107-114.
[27] Sadrzadeh SM and Bozorgmehr J. Haptoglobin phenotypes in health and disorders. Am J Clin Pathol 2004; 121 Suppl: S97-104.
[28] Kristiansen M, Graversen JH, Jacobsen C, Sonne O, Hoffman HJ, Law SK and Moestrup SK. Identification of the haemoglobin scavenger receptor. Nature 2001; 409: 198-201.
[29] Graversen JH, Madsen M and Moestrup SK. CD163: a signal receptor scavenging haptoglobin-hemoglobin complexes from plasma. Int J Biochem Cell Biol 2002; 34: 309-314.
[30] Melamed-Frank M, Lache O, Enav BI, Szafranek T, Levy NS, Ricklis RM and Levy AP. Structure-function analysis of the antioxidant properties of haptoglobin. Blood 2001; 98: 3693-3698.
[31] Vardi M and Levy AP. Is it time to screen for the haptoglobin genotype to assess the cardiovascular risk profile and vitamin E therapy respon-

siveness in patients with diabetes? Curr Diab Rep 2012; 12: 274-279.
[32] Costa-Mallen P, Zabetian CP, Hu SC, Agarwal P, Yearout D and Checkoway H. Smoking and haptoglobin phenotype modulate serum ferritin and haptoglobin levels in Parkinson disease. J Neural Transm (Vienna) 2016; 123: 1319-1330.
[33] Costa-Mallen P, Zabetian CP, Agarwal P, Hu SC, Yearout D, Samii A, Leverenz JB, Roberts JW and Checkoway H. Haptoglobin phenotype modifies serum iron levels and the effect of smoking on Parkinson disease risk. Parkinsonism Relat Disord 2015; 21: 1087-1092.
[34] Costacou T, Ferrell RE, Ellis D and Orchard TJ. Haptoglobin genotype and renal function decline in type 1 diabetes. Diabetes 2009; 58: 2904-2909.
[35] Lioupis C, Barbatis C, Drougou A, Koliaraki V, Mamalaki A, Klonaris C, Georgopoulos S, Andrikopoulos V and Bastounis E. Association of haptoglobin genotype and common cardiovascular risk factors with the amount of iron in atherosclerotic carotid plaques. Atherosclerosis 2011; 216: 131-138.
[36] Ravona-Springer R, Heymann A, Schmeidler J, Guerrero-Berroa E, Sano M, Preiss R, Koifman K, Hoffman H, Levy A, Silverman JM and Schnaider-Beeri M. Haptoglobin 1-1 genotype is associated with poorer cognitive functioning in the elderly with type 2 diabetes. Diabetes Care 2013; 36: 3139-3145.
[37] Staals J, Pieters BM, Knottnerus IL, Rouhl RP, van Oostenbrugge RJ, Delanghe JR and Lodder J. Haptoglobin polymorphism and lacunar stroke. Curr Neurovasc Res 2008; 5: 153-158.
[38] Rouhl RP, van Oostenbrugge RJ, Damoiseaux JG, Debrus-Palmans LL, Theunissen RO, Knottnerus IL, Staals JE, Delanghe JR, Tervaert JW and Lodder J. Haptoglobin phenotype may alter endothelial progenitor cell cluster formation in cerebral small vessel disease. Curr Neurovasc Res 2009; 6: 32-41.
[39] Wong KT, Grove JS, Grandinetti A, Curb JD, Yee M, Blanchette P, Ross GW and Rodriguez BI. Association of fibrinogen with Parkinson disease in elderly Japanese-American men: a prospective study. Neuroepidemiology 2010; 34: 50-54.
[40] Kamath S and Lip GY. Fibrinogen: biochemistry, epidemiology and determinants. Qjm 2003; 96: 711-729.
[41] Mila S, Albo AG, Corpillo D, Giraudo S, Zibetti M, Bucci EM, Lopiano L and Fasano M. Lymphocyte proteomics of Parkinson's disease patients reveals cytoskeletal protein dysregulation and oxidative stress. Biomark Med 2009; 3: 117-128.
[42] Ugarova TP and Yakubenko VP. Recognition of fibrinogen by leukocyte integrins. Ann N Y Acad Sci 2001; 936: 368-385.
[43] Mosesson MW. Fibrinogen gamma chain functions. J Thromb Haemost 2003; 1: 231-238.
[44] Chen H, O'Reilly EJ, Schwarzschild MA and Ascherio A. Peripheral inflammatory biomarkers and risk of Parkinson's disease. Am J Epidemiol 2008; 167: 90-95.
[45] Hald A, Van Beek J and Lotharius J. Inflammation in Parkinson's disease: causative or epiphenomenal? Subcell Biochem 2007; 42: 249-279.
[46] Klegeris A, McGeer EG and McGeer PL. Therapeutic approaches to inflammation in neurodegenerative disease. Curr Opin Neurol 2007; 20: 351-357.
[47] Xu J, Wang G, Fu D, Su N, Wang L, Gao F and Guo N. High-resolution color doppler ultrasound examination and related risk factor analysis of lower extremity vasculopathy in type 2 diabetes patients. Genet Mol Res 2015; 14: 3939-3947.
[48] Singh VP, Bali A, Singh N and Jaggi AS. Advanced glycation end products and diabetic complications. Korean J Physiol Pharmacol 2014; 18: 1-14.
[49] van den Herik EG, Cheung EY, de Lau LM, den Hertog HM, Leebeek FW, Dippel DW, Koudstaal PJ and de Maat MP. gamma'/total fibrinogen ratio is associated with short-term outcome in ischaemic stroke. Thromb Haemost 2011; 105: 430-434.
[50] Mingazov ER and Ugrumov MV. Gene expression of proteins of the vesicle cycle in dopaminergic neurons in modeling of Parkinson's disease. Dokl Biochem Biophys 2016; 468: 206-208.
[51] Mullard AJ, Reeves MJ, Jacobs BS, Kothari RU, Birbeck GL, Maddox K, Stoeckle-Roberts S and Wehner S. Lipid testing and lipid-lowering therapy in hospitalized ischemic stroke and transient ischemic attack patients: results from a statewide stroke registry. Stroke 2006; 37: 44-49.
[52] Sodero AO, Vriens J, Ghosh D, Stegner D, Brachet A, Pallotto M, Sassoe-Pognetto M, Brouwers JF, Helms JB, Nieswandt B, Voets T and Dotti CG. Cholesterol loss during glutamate-mediated excitotoxicity. EMBO J 2012; 31: 1764-1773.
[53] Lou X and Shin YK. SNARE zippering. Biosci Rep 2016; 36.
[54] Martin JA, Hu Z, Fenz KM, Fernandez J and Dittman JS. Complexin has opposite effects on two modes of synaptic vesicle fusion. Curr Biol 2011; 21: 97-105.
[55] Lin MY, Rohan JG, Cai H, Reim K, Ko CP and Chow RH. Complexin facilitates exocytosis and synchronizes vesicle release in two secretory model systems. J Physiol 2013; 591: 2463-2473.
[56] Kaeser-Woo YJ, Yang X and Sudhof TC. C-terminal complexin sequence is selectively

required for clamping and priming but not for Ca2+ triggering of synaptic exocytosis. J Neurosci 2012; 32: 2877-2885.

[57] Ramos-Miguel A, Sawada K, Jones AA, Thornton AE, Barr AM, Leurgans SE, Schneider JA, Bennett DA and Honer WG. Presynaptic proteins complexin-I and complexin-II differentially influence cognitive function in early and late stages of Alzheimer's disease. Acta Neuropathol 2017; 133: 395-407.

[58] Wragg RT, Snead D, Dong Y, Ramlall TF, Menon I, Bai J, Eliezer D and Dittman JS. Synaptic vesicles position complexin to block spontaneous fusion. Neuron 2013; 77: 323-334.